Nuclear magnetiresonance and X-ray studies on micellar aggregates of sodium deoxycholate

ARTICLE *in* THE JOURNAL OF PHYSICAL CHEMISTRY · NOVEMBER 1984

Impact Factor: 2.78 · DOI: 10.1021/j150667a052

of the unidimensional objects, we guess that a somewhat different approach would be required in the case of very stiff rodlike micelles (see, for instance, the recent paper of Gelbart and Ben Shaul[9]).

Acknowledgment. B. Brun and G. Haouche (Laboratoire de Physico-Chimie des Systèmes Polyphasés Montpellier) are gratefully acknowledged for making the viscosimeter available to us and for helpful technical assistance.

Registry No. CPBr, 140-72-7; CPCl, 123-03-5.

Nuclear Magnetic Resonance and X-ray Studies on Micellar Aggregates of Sodium Deoxycholate

G. Conte,† R. Di Blasi,† E. Giglio,*‡ A. Parretta,† and N. V. Pavel†

Laboratori Ricerche di Base ASSORENI, Monterotondo, Roma, Italy, and Dipartimento di Chimica, Università di Roma, 00185 Roma, Italy *(Received: March 2, 1984; In Final Form: June 1, 1984)*

X-ray studies on crystals of sodium and rubidium deoxycholates (NaDC and RbDC, respectively) and on a macromolecular fiber of NaDC provide a reasonable helical model for describing the structure of the NaDC micellar aggregates in aqueous solutions, at least within a certain concentration range and at natural pH. ^1H and ^{13}C NMR measurements have been performed to check the validty both of this model and of a previous model, currently accepted in the literature. The results satisfactorily agree with the helical model which is characterized by an interior part formed by Na^+ ions and water molecules, arranged as in a liquidlike structure, and by an outer surface covered by nonpolar groups. A very complicated network of hydrogen bonds among water molecules and hydroxyl and carboxyl groups of deoxycholate anions stabilizes the helix together with $Na^+ \cdots H_2O$ ion–dipole and $Na^+ \cdots COO^-$ ion–ion interactions. Therefore, hydrophobic interactions can occur among helices, but are negligible in the formation of the micelle. The investigation of the solubilization of some hydrocarbons by NaDC aqueous solutions indicates that the solubilization sites are mainly located at the boundary between the micelles and the bulk aqueous phase, near the C_{19} methyl group.

Introduction

The alkali-metal salts of 3α,12α-dihydroxy-5β-cholan-24-oic acid (deoxycholic acid, DCA) associate in aqueous solutions to give micellar aggregates.[1] DCA (Figure 1) presents both an arched shape, mainly due to the cis fusion of the A and B rings, and two faces, one polar, characterized by two secondary hydroxyl groups at C_3 and C_{12}, and the other nonpolar, characterized by two angular methyl groups at C_{10} and C_{13}. A short aliphatic chain, with another methyl group at C_{20}, protrudes from ring D at C_{17} and ends in a carboxyl group.

The geometry of this molecule, together with the permissible conformations of the side chain and ring D, is now well-known from the solution of several crystal structures of DCA inclusion compounds.[2,3] The side chain can assume a "trans" or "gauche" state with a C_{17}–C_{20}–C_{22}–C_{23} dihedral angle of about 190° and 60°, respectively, according to the convention of Klyne and Prelog.[4] Moreover, the structure of a monoclinic crystal of rubidium deoxycholate (RbDC) monohydrate shows that the deoxycholate anion (DCA^-) holds the same geometry of DCA, with a gauche side chain and a ring D conformation close to the half-chair symmetry.[5]

In all the crystals studied so far the DCA molecules and the DCA^- anions give rise to two types of structures, the bilayer and the helix. Some types of bilayers have been observed in orthorhombic and tetragonal crystals of the DCA inclusion compounds[2] as well as in monoclinic crystals of RbDC.[5] The helix has been found in hexagonal crystals of DCA inclusion compounds.[2] It is interesting to note that hydrogen bonding plays a leading role in the formation of both structures.

The sodium salt of DCA (NaDC) is one of the most studied bile salts and forms molecular aggregates in aqueous solution capable of solubilizing many water-insoluble compounds,[6-12] some of which are biologically important, such as cholesterol,[6,7] phospholipids,[8] sequential copolypeptides,[10] and tingenone.[12] The size of the molecular aggregates depends on many parameters, for example, ionic strength, pH, temperature, and pressure.[1] The NaDC aggregates can grow under suitable conditions to give a gel formed by helical macromolecules,[13,14] the gelation of NaDC being favored by lowering the pH[14] and the temperature[15] and by raising the ionic strength[14] and the pressure.[15] Some authors invoke hydrogen bonding as the driving force in the aggregation process on the basis of pH, pNa, density, and conductivity measurements.[15-18] Moreover, the aggregation of NaDC has been investigated by means of viscosity, density, light scattering, circular dichroism, and solubilization of cholesterol measurements, it being pointed out that in aqueous solution four concentration regions exist in which are present NaDC monomers, oligomers (dimers, trimers, tetramers, ...), polymer-like (helical) aggregates, and nearly spherical aggregates.[19]

†Laboratori Ricerche di Base ASSORENI.
‡Università di Roma.

(1) Small, D. M. "The Bile Acids"; Nair, P. P., Kritchevsky, D., Eds.; Plenum Press: New York, 1971; Chapter 8, pp 249–356.
(2) Giglio, E. *J. Mol. Struct.* **1981**, *75*, 39 and references quoted therein.
(3) Giglio, E.; Quagliata, C. *Acta Crystallogr. Sect. B* **1975**, *B31*, 743.
(4) Klyne, W.; Prelog, V. *Experientia* **1960**, *16*, 521.
(5) Coiro, V. M.; Giglio, E.; Morosetti, S.; Palleschi, A. *Acta Crystallogr., Sect. B* **1980**, *B36*, 1478.
(6) Small, D. M.; Bourges, M.; Dervichian, D. G. *Nature (London)* **1966**, *211*, 816.
(7) Bourges, M.; Small, D. M.; Dervichian, D. G. *Biochim. Biophys. Acta* **1967**, *144*, 189.
(8) Philippot, J. *Biochim. Biophys. Acta* **1971**, *225*, 201.
(9) Fontell, K. *Kolloid Z. Z. Polym.* **1972**, *250*, 333.
(10) Corsi, E.; D'Alagni, M.; Giglio, E. *Polymer* **1976**, *17*, 259.
(11) Thomas, D. C.; Christian, S. D. *J. Colloid Interface Sci.* **1981**, *82*, 430.
(12) Campanelli, A. R.; D'Alagni, M.; Giglio, E.; Marini-Bettolo, G. B. *Farmaco, Ed. Prat.* **1981**, *36*, 30.
(13) Rich, A.; Blow, D. M. *Nature (London)* **1958**, *182*, 423.
(14) Blow, D. M.; Rich, A. *J. Am. Chem. Soc.* **1960**, *82*, 3566.
(15) Sugihara, G.; Ueda, T.; Kaneshina, S.; Tanaka, M. *Bull. Chem. Soc. Jpn.* **1977**, *50*, 604.
(16) Sugihara, G.; Tanaka, M. *Bull. Chem. Soc. Jpn.* **1976**, *49*, 3457.
(17) Oakenfull, D. G.; Fischer, L. R. *J. Phys. Chem.* **1977**, *81*, 1838.
(18) Oakenfull, D. G.; Fischer, L. R. *J. Phys. Chem.* **1978**, *82*, 2443.
(19) Murata, Y.; Sugihara, G.; Nishikido, N.; Tanaka, M. In "Solution Behavior of Surfactants: Theoretical and Applied Aspects"; Mittal, K. L., Fendler, E. J., Eds.; Plenum Press: New York, 1982; Vol. 1, pp 611–28.

0022-3654/84/2088-5720$01.50/0

TABLE I: Crystallographic Data of NaDC and RbDC Crystals and of the NaDC Fiber

	a, Å	b, Å	c, Å	α, deg	β, deg	γ, deg	SG	d_x, g cm^{-3}	d_m, g cm^{-3}	mp, K
NaDC crystal	34.56	34.56	11.75	90	90	120	$P6_5$	1.20[a]	1.21	574–576
RbDC crystal	19.83	19.31	11.59	90	90	116.7	$P2_1$	1.35[b]	1.35	594–596
NaDC fiber	36.2	36.2	51.4	90	90	120		1.20[c]	1.20	566–568

[a] Value calculated for 18 NaDC and 72 H_2O molecules in the unit cell. [b] Value calculated for 6 RbDC and 20 H_2O molecules in the unit cell. [c] Value calculated for 87 NaDC and 348 H_2O molecules in the unit cell.

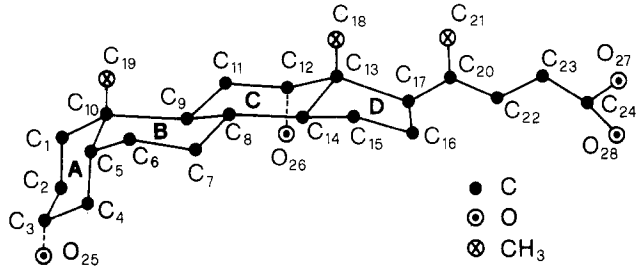

Figure 1. Atomic numbering of DCA. The hydrogen atoms are omitted.

It has been postulated that NaDC forms small micelles of cylindrical shape, containing up to about 10 monomers ("primary" micelles) and built up by "back-to-back" hydrophobic interactions arising from the nonpolar faces of the NaDC molecules, whereas the polar faces are oriented toward the solvent molecules.[20,21] Moreover, the primary micelles, which have hydrophilic exterior surfaces, can associate under proper conditions by means of hydrogen bonds to give larger "secondary" micelles.

The only direct evidence for this currently accepted model is based on a proton NMR investigation of aqueous solutions of sodium cholate and deoxycholate.[22] The NMR spectra showed, on micelle formation, a differential broadening of the signals from the C_{18} methyl group, belonging to the nonpolar face of the steroid nucleus, compared with those from the C_{12} proton, assigned to the polar face.

A wide-angle X-ray diffraction study has been undertaken on some NaDC phases which seem strictly related to each other. These phases are (α) aqueous solutions of NaDC above the critical micelle concentration (cmc), (β) the NaDC gel, (γ) the fiber which can be drawn from NaDC aqueous solutions, and (δ) hexagonal crystals of NaDC, belonging to the space group $P6_5$, obtainable from aqueous solutions of NaDC by slow evaporation or from γ by aging.[23] The results so far acquired indicate that the β, γ, and δ phases are formed by helices of NaDC molecules held together mainly by hydrogen bonds, Na^+---DCA$^-$ Coulombic interactions, and Na^+---H_2O ion–dipole interactions. The transformation $\alpha \rightarrow \beta$ seems to be continuous, as mentioned previously, so that it is reasonable to suppose that in the α phase the NaDC aggregates are also helical, at least within a concentration range far from the cmc.

This hypothesis is supported by the X-ray diffraction patterns of the α, β, γ, and δ phases, which show maxima of intensity in the same ϑ regions. Moreover, the structure of the NaDC helix has been confirmed by studying another monoclinic crystal of RbDC–water (3:10),[24] which is strictly related to the NaDC hexagonal crystal.[23,24] Since the model of the primary and secondary micelles is incompatible with these findings, we have accomplished NMR and X-ray studies in order to verify both the results of Small, Penkett, and Chapman[22] (hereafter abbreviated to SPC) and the validity of our helical model.

Experimental Section

Materials. NaDC purchased from Fluka and Calbiochem was recrystallized 4 times from a mixture of water and acetone and its purity was confirmed by thin-layer chromatography. The hexagonal crystals so obtained contain four water molecules for each NaDC molecule. Their composition was checked by X-ray, density, spectropolarimetric, thermogravimetric, and elemental analysis measurements. The presence of acetone was ruled out by means of NMR spectra. The NaDC fibers were prepared as described in ref 23. Twice-distilled water was used through all the experiments. D_2O (≥99.9 atom % D) and CD_3OD (≥99.5 atom % D) were Merck and Wilmad, respectively. Acetone, phenanthrene, *p*-xylene, styrene, *trans*-2-butene, and 2,3-dimethyl-2-butene were reagent grade. The NaDC aqueous solutions containing phenanthrene, *p*-xylene, styrene, and 2,3-dimethyl-2-butene were prepared by adding to the NaDC solutions the solid or liquid compound and, then, by shaking for several hours. *trans*-2-Butene was bubbled at 10 °C for 1 h into the NaDC aqueous solution. The NaDC/solubilizate molar ratio was determined by NMR quantitative analysis.

NMR Measurements. ^1H NMR spectra were recorded by means of a Varian XL-100 pulsed FT spectrometer, equipped with a 16 K Varian 620i computer, operating at 100.1 MHz. ^{13}C NMR spectra were obtained on a Bruker WH 270 spectrometer at 67.88 MHz. Me_4Si dissolved in CCl_4 was used as an external standard for ^1H spectra. ^{13}C chemical shifts were measured with respect to Me_4Si by using dioxane as an internal standard. All spectra were recorded with an internal lock signal from deuterium of D_2O and CD_3OD at 30 ± 2 °C if not otherwise specified.

The usual experimental parameters were as follows. ^1H spectra: 1000-Hz sweep width; acquisition time, 4 s; a pulse width of 17 μs; 1000–2000 transients; chemical shift measurements were accurate to 0.25 Hz. ^{13}C spectra: 15 000-Hz sweep width; acquisition time, 0.5 s; additional delay, 0.3 s; a pulse width of 8 μs; 500–42 000 transients. Chemical shift measurements were accurate to 0.03 ppm. All the spectra were recorded under proton noise decoupling.

X-ray Measurements. Weissenberg, precession, and Debye-Scherrer cameras were used to collect X-ray data of NaDC crystals and fibers by means of Cu Kα radiation; 3230 independent reflections with $I > 3\sigma(I)$ of a NaDC·4H_2O hexagonal crystal were recorded up to $2\vartheta = 110°$ by the ω-scan mode on a Syntex $P2_1$ automated diffractometer with graphite-monochromatized Cu Kα radiation; 3057 independent reflections with $I > 2\sigma(I)$ of a 3RbDC·10H_2O monoclinic crystal were recorded up to $2\vartheta = 140°$ by the $\vartheta/2\vartheta$-scan mode on a Siemens AED automated diffractometer with Cu Kα Ni-filtered radiation.

Results and Discussion

Some relevant X-ray data are given in Table I for crystals of NaDC·4H_2O and 3RbDC·10H_2O together with the NaDC macromolecular fiber.[23,24] Unfortunately, attempts to determine the NaDC crystal structure were unsuccessful. However, Patterson and minimum residual analyses confirmed that in the crystal there are helices, very likely identical, around the 6_5 and 3_2 helical axes with radii of about 10 Å. Six NaDC molecules are packed along *c* with their C_9–C_{13} middle points about 8.6 Å from the 6_5 and 3_2 axes, whereas the interior of each helix is filled with Na^+ ions and water molecules. In order to solve this structure at the atomic level a nearly isostructural compound, containing heavier Rb^+ ions, was prepared. The repeat of six DCA$^-$ anions along the helical axis *c* is nearly equal to that of NaDC (11.59 vs. 11.75 Å). The C_9–C_{13} middle points of the three independent DCA$^-$ anions are 7.4, 8.0, and 8.6 Å from the 2_1 helical axis. The RbDC unit cell has corners in the *ab* plane corresponding approximately to the points (0,0), ($^2/_3$,$^1/_3$), ($^1/_3$,$^2/_3$), and ($-^1/_3$,$^1/_3$) of the NaDC unit cell. Figures 2 and 3 show in the *ab* plane the approximate

(20) Small, D. M. *Adv. Chem. Ser.* **1968**, *No. 84*, 31.
(21) Carey, M. C.; Small, D. M. *Arch. Intern. Med.* **1972**, *130*, 506.
(22) Small, D. M.; Penkett, S. A.; Chapman, D. *Biochim. Biophys. Acta* **1969**, *176*, 178.
(23) Campanelli, A. R.; Ferro, D.; Giglio, E.; Imperatori, P.; Piacente, V. *Thermochim. Acta* **1983**, *67*, 223.
(24) Campanelli, A. R.; Candeloro De Sanctis, S.; Giglio, E.; Petriconi, S. *Acta Crystallogr., Sect. C* 1984, *C40*, 631.

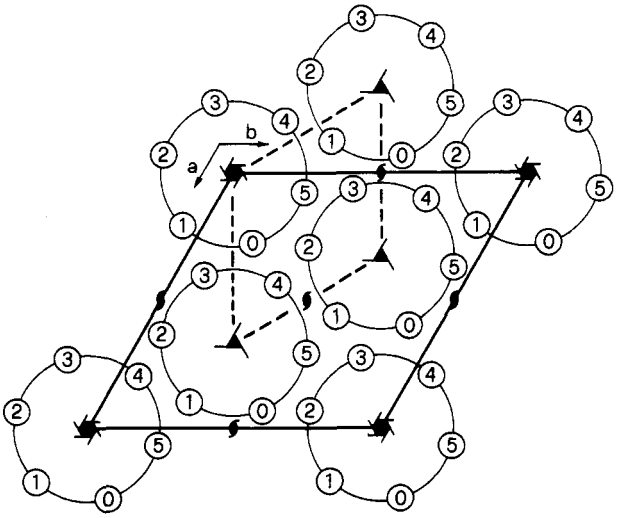

Figure 2. Schematic drawing of the NaDC crystal packing viewed along *c*. The small and large open circles represent a DCA^- anion and a helix, respectively. The figures inside the small open circles indicate their height on *c* in *c*/6 units. The broken lines show the approximate *ab* plane of RbDC.

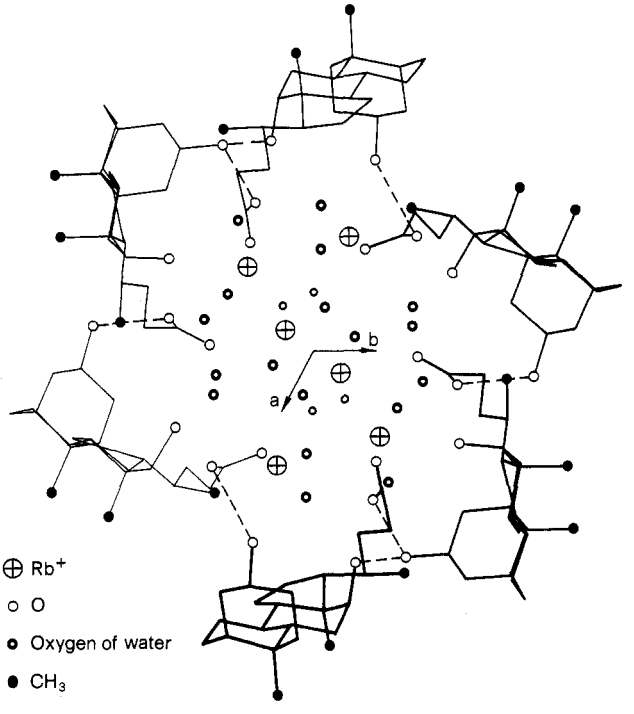

Figure 3. View of a RbDC–water (3:10) helix along *c*. Only the hydrogen bonds among DCA^- anions are indicated by broken lines. The thin circles represent oxygen atoms of water molecules with occupation site of 0.5.

relation between the NaDC and RbDC unit cells and the projection of the RbDC helix, respectively. Thus, the RbDC helix can be obtained by slight movements from the sixfold helix of NaDC, of which the RbDC helix keeps the screw sense. It is interesting to note that the atomic coordinates, appropriately transformed, of the DCA^- anion, drawn with the thickest line in Figure 3, correspond to a minimum of the *R* factor (0.46) for 3230 observed reflections of NaDC, without including Na^+ ions and water molecules and with an overall temperature factor. Work is in progress to solve the NaDC crystal structure.

The X-ray pattern of the NaDC fiber is a characteristic helical pattern and can be interpreted by a hexagonal cell with the parameters of Table I. The equatorial spacings are close to those of the crystal and, therefore, a similar packing of helices can be expected. However, the very high *c* value, slightly different from

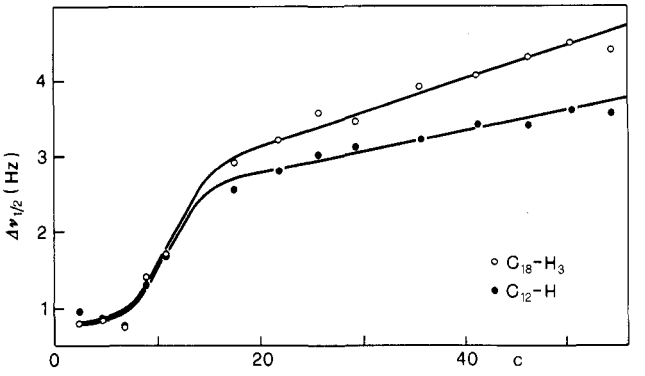

Figure 4. Half-height line width of C_{12}–H and C_{18}–H_3 as a function of NaDC molar concentration multiplied by 10^3. C_{12}–H and C_{11}–H_2 have been decoupled.

that reported by Rich and Blow,[13] points out that the helix of the crystal is not equal to that of the fiber. Three intense layer lines near the meridian and a strong arc occur at 7.4, 6.4, 5.7, and 3.42 Å and correspond to the 7th, 8th, 9th and 15th layer lines, respectively (no splitting of the fourth layer line[13] is observed). The measured density agrees with three helices, each one formed by 29 ($NaDC \cdot 4H_2O$), in the unit cell. Thus, the helix is generated by rotating 62.07° and by translating 1.77 Å along *c* a $NaDC \cdot 4H_2O$ unit.

The corresponding values of the crystal, 30 ($NaDC \cdot 4H_2O$), 60°, and 1.96 Å, justify the easy fiber → crystal transition by aging and support the hypothesis that the helix of the fiber can be obtained from that of the crystal by means of slight changes.

NaDC has been studied by proton,[22,25] carbon-13,[25-27] and deuteron[28] NMR together with its association with lecithin,[22,28] some aromatic hydrocarbons,[26,29,30] and cholesterol.[31]

^1H NMR spectra of NaDC in D_2O and CD_3OD were recorded, the concentration being 5 g/100 mL, the same as that used by SPC. Some relevant chemical shifts and half-height line widths measured at 30 °C agree with those observed by SPC at 33.4 °C. The sharper and more resolved peaks found in CD_3OD, as compared with those in D_2O, confirm the results obtained by Small[22] by means of equilibrium ultracentrifugation and vapor pressure osmometry which indicate that the NaDC molecules are singly dispersed in methanol. Thus, the C_{12}–H signal in CD_3OD, owing to the coupling with the neighboring C_{11}–H_2 methylenic group, presents a 1:2:1 triplet structure which is replaced by a broad singlet in D_2O.

The half-height line width of this singlet markedly changes if C_{12}–H and C_{11}–H_2 are decoupled. Thus, the constant line width observed as a function of concentration by SPC, who did not take into account this decoupling, cannot be claimed as evidence that the polar part of DCA^- is on the outside of the micelle in contact with the aqueous environment.[22] In fact, the trend of the C_{12}–H half-height line width vs. the NaDC concentration, shown in Figure 4 together with that of C_{18}–H_3 for comparison, indicates that no difference exists between a proton belonging to the DCA^- polar face (or, more precisely, lying in a plane passing approximately halfway to the polar and nonpolar faces) and the protons of a group belonging to the nonpolar face. Therefore, the broadening of the C_{18}–H_3 signal cannot be taken as an argument in favor of the association of the nonpolar faces in the formation of the primary micelles, since similar reasoning leading one to hypothesize the association of the polar faces (or, at least, of the C_{12}–H groups)

(25) Paul, R.; Mathew, M. K.; Narayanan, R.; Balaram, P. *Chem. Phys. Lipids* **1979**, *25*, 345.
(26) Leibfritz, D.; Roberts, J. D. *J. Am. Chem. Soc.* **1973**, *95*, 4996.
(27) Murata, Y.; Sugihara, G.; Fukushima, K.; Tanaka, M.; Matsushita, K. *J. Phys. Chem.* **1982**, *86*, 4690.
(28) Fung, B. M.; Peden, M. C. *Biochim. Biophys. Acta* **1976**, *437*, 273.
(29) Menger, F. M.; Rhee, J.-U.; Mandell, L. *J. Chem. Soc., Chem. Commun.* **1973**, 918.
(30) Fung, B. M.; Thomas, L. *Chem. Phys. Lipids* **1979**, *25*, 141.
(31) Sugihara, G.; Yamakawa, K.; Murata, Y.; Tanaka, M. *J. Phys. Chem.* **1982**, *86*, 2784.

TABLE II: $-\Delta\delta$ of NaDC Protons in the Presence of Some Probes[a]

solubilizate (R)	$-\Delta\delta$, Hz			
	C_3–H	C_{12}–H	C_{18}–H_3	C_{19}–H_3
p-xylene (3.6)	2.6	3.0	3.4	9.6
phenanthrene (16.0)	0.0	1.8	1.6	5.6
styrene (3.8)	*b*	3.0	4.0	10.0
2,3-dimethyl-2-butene (12.0)	*b*	0.5	1.0	2.0
trans-2-butene (4.0)	*b*	0.0	0.0	0.5

[a] The values refer to upfield shifts. [b] Undetermined value owing to a large signal and a low signal-to-noise ratio.

can be made. A reasonable explanation can be provide by a helical model of the type shown in Figure 3. The helix is characterized by an interior filled with Rb^+ (or Na^+) ions and water molecules which give rise to ion–dipole interactions. The alkali-metal ions are engaged in Coulombic interactions with the carboxylic groups, whereas the water molecules form hydrogen bonds among them and with the hydroxylic and carboxylic groups of the DCA^- anions. These interactions, together with the hydrogen bonds among DCA^- anions shown in Figure 3, stabilize the helix which has the outer surface covered by nonpolar groups, C_{19} and C_{18} being in this order the most protruding. Thus, the increasing of $\Delta\nu_{1/2}$ with the NaDC concentration may be explained both for C_{12}–H with the growth of the micelle (helix) and, hence, with the formation of hydrogen bonds in which the O_{26}–H hydroxyl group is engaged and for C_{18}–H_3 with hydrophobic interactions which are more probable among helices when the number of helices and the helical size increase.

In order to establish if the nonpolar face of DCA^- is oriented toward the aqueous medium, ^1H NMR spectra of NaDC solutions above the cmc and containing some solubilizates have been recorded. Especially aromatic probes have been considered to study their sites of solubilization by monitoring the ring current induced alterations in the chemical shifts of the NaDC protons, taking into account that in the literature such probes are reported to be located at the interface of ionic micelles near the headgroups.[32] Since the outer surfaces of the helix and the probes are both nonpolar, the micelle–solubilizate interactions are favored. We have obtained the data of Table II, where the probe-induced change in the NMR chemical shifts of NaDC is indicated with $\Delta\delta$ and the NaDC/probe molar ratio with R. Some results concerning nonaromatic molecules with double bonds are reported for comparison. The effects observed on C_{19}–H_3 are greater than those on the other protons. This is meaningful since C_{19}–H_3 is the outermost group of the helix, and, hence, the group which can interact more easily with the solubilizate, although the separation between two adjacent DCA^- in the helix is so large that also the hydroxyl groups could be approached by the probes. Assuming the SPC model the probe must be located in the interior of the micelle, but there is no reason to invoke for C_{19}–H_3 a different behavior than for C_{18}–H_3, which presents $\Delta\delta$ very near those of C_{12}–H. Small effects are given by *trans*-2-butene and 2,3-dimethyl-2-butene, thus supporting the view that the greatest $\Delta\delta$ of C_{19}–H_3 are due to the ring current of the aromatic compounds. On the other hand, the crystal structures of the DCA inclusion compounds show that, when the guest molecule is aromatic, the strongest host–guest interactions are of the polarization bonding type, involving the methyl groups of DCA and the π charge cloud of the aromatic molecule.[33,34]

The change of $\Delta\delta$ as a function of the solubilizate/NaDC molar ratio ($1/R$) is reported in Figure 5 for *p*-xylene. The results indicate that, up to a 1:3.4 molar ratio, the variation is monotonic and undramatic for C_3–H, C_{12}–H, C_{18}–H_3, and C_{19}–H_3. The insolubility of *p*-xylene in water suggests that all the probe is practically micelle bound with most of its molecules near C_{19}–H_3,

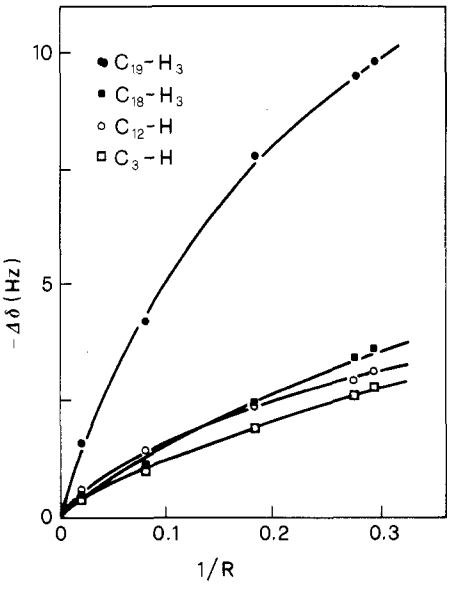

Figure 5. $-\Delta\delta$ vs. $1/R$ for some NaDC protons in the NaDC–*p*-xylene aqueous solutions.

since the signal of this methyl group experiences the greatest perturbation as found also by Menger et al.[29] Moreover, some authors[9,26] have reported a *p*-xylene/NaDC molar ratio up to about 1:2, so that it seems very difficult to accommodate in the interior of the SPC micelle so many molecules of *p*-xylene (about half of the aggregation number) without changing dramatically the structure of the micelle. On the contrary, the helical model, with the *p*-xylene molecules located at the outer surface of the helix, can account for a molar ratio as high as 1:1 (one *p*-xylene molecule for each C_{19} methyl group at least, see Figure 3). Moreover, the study by NMR and circular dichroism techniques of the interaction between an optical probe, (+)-*trans*-2-chloro-5-methylcyclohexanone, and NaDC micelles can be taken into account.[35] The results show that the probe, which is sensitive to the nature of the medium surrounding it,[36–38] is dipped in the bulk water phase and interacts with the NaDC nonpolar face again up to a molar ratio of about 1:2. This finding supports, also in the case of a nonaromatic probe, the helical model of the micelle and the probe–micelle interaction mode postulated in this paper.

The NaDC micelle formation has been studied as a function of the NaDC concentration by means of ^{13}C NMR chemical shift, surface tension, and partial molal volume measurements by Murata et al.,[27] hereafter indicated as MSFTM. The NaDC aqueous solutions investigated were at pH 7.8 and contained polymer-like aggregates not observed above pH 8.[11,21,39–41] From ^{13}C NMR chemical shifts, measured approximately within the NaDC concentration range 5×10^{-3}–5×10^{-2} M, MSFTM concluded that the polymer-like aggregate presents a somewhat ordered structure characterized by intermolecular O_{25}–H---COO^- hydrogen bonds together with partially hydrophobic interactions (back-to-back). This interpretation is based on an upfield shift of about 0.6 ppm for C_3 and C_{24} and a downfield shift of about 0.5 and 0.4 ppm for C_{18} and C_{19}, respectively, with increasing NaDC concentration. On the other hand, C_{10} and C_{13}, chosen as representatives of the steroid ring, and C_{21} show small changes in their chemical shifts, which means that they are only slightly

(32) Ganesh, K. N.; Mitra, P.; Balasubramanian, D. *J. Phys. Chem.* **1982**, *86*, 4291 and references quoted therein.
(33) Candeloro De Sanctis, S.; Giglio, E.; Pavel, V.; Quagliata, C. *Acta Crystallogr., Sect. B* **1972**, *B28*, 3656.
(34) Coiro, V. M.; Giglio, E.; Mazza, F.; Pavel, N. V.; Pochetti, G. *Acta Crystallogr., Sect. B* **1982**, *B38*, 2615.
(35) D'Alagni, M.; Forcellese, M. L.; Giglio, E., submitted for publication in *Colloid Polym. Sci.*
(36) Djerassi, C.; Geller, L. E.; Eisenbraun, E. J. *J. Org. Chem.* **1960**, *25*, 1.
(37) Moscowitz, A.; Wellman, K.; Djerassi, C. *J. Am. Chem. Soc.* **1963**, *85*, 3515.
(38) Menger, F. M.; Boyer, B. J. *J. Am. Chem. Soc.* **1980**, *102*, 5936.
(39) Djavanbakht, A.; Kale, K. M.; Zana, R. *J. Colloid Interface Sci.* **1977**, *59*, 139.
(40) Chang, Y.; Cardinal, J. R. *J. Pharm. Sci.* **1978**, *67*, 994.
(41) Vandnere, M.; Matarajan, R.; Lindenbaum, S. *J. Phys. Chem.* **1980**, *84*, 1900.

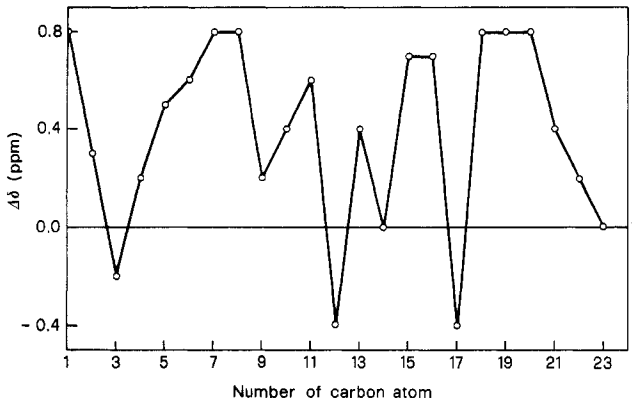

Figure 6. $\Delta\delta$ of the various NaDC carbon atoms by increasing the concentration. Positive and negative values mean downfield and upfield shifts, respectively.

affected in the breakdown of the polymer-like aggregates, occurring at lower NaDC concentration, into smaller aggregates. In this connection we have measured ^{13}C NMR chemical shifts for six NaDC aqueous solutions (concentrations: 2.4×10^{-3}, 6.2×10^{-3}, 1.5×10^{-2}, 2.5×10^{-2}, 1.1×10^{-1}, and 2.0×10^{-1} M) at 40 °C and natural pH, less than 8 for the first two solutions and greater than 8 for the other ones.[16] The trend of the chemical shift generally agrees with that found by MSFTM, but C_3 and C_{12} must be interchanged if the assignment of Leibfritz et al.[26] is accepted. Only the final differences $\Delta\delta$ in the chemical shift of the carbon atoms passing from a concentration of 2.4×10^{-3} to 2.0×10^{-1} M are shown in Figure 6. C_{24} is not given since its spectral peak lies far from the others in a downfield region not recorded by us. The $\Delta\delta$ values of −0.2 and −0.4 for C_3 and C_{12} and 0.8 for both C_{18} and C_{19} are comparable with those of MSFTM. The last four solutions examined do not contain the polymer-like aggregate since their pH is greater than 8 and small-angle X-ray data on these solutions (our unpublished results) confirm that the aggregation number is very low (around 10). On the other hand, the polymer-like aggregates are present in the first two solutions (pH much less than 8) and, therefore, we also detect the change polymer-like aggregates → smaller aggregates. However, this change occurs with a decrease in the mobility of the C_{18} and C_{19} protons (see Figure 4 for C_{18}) so that the downfield shifts of the methyl groups could be attributed to a steric crowding effect as observed by other authors.[42,43] Moreover, C_{10} and C_{13}, together with many other carbon atoms of the steroid ring, give downfield shifts (Figure 6), which could indicate that the stiffness of the NaDC skeleton depends on the NaDC concentration, at variance with the results of MSFTM. If the polymer-like aggregate is described by the helical model,[14] the enhancement of the steric crowding effect, regarding the methyl groups, can be explained by the increasing of the number of helices with the concentration if the nonpolar groups, belonging to different helices, interact among them.

The upfield shifts of C_3, C_{12}, and C_{24}, increasing with the NaDC concentration, correspond, following the MSFTM interpretation, to the decrease in the steric crowding and/or the increase in the electron density due to the breakdown of hydrogen bonding. We believe that it is difficult to establish if the steric crowding causes an upfield[44] or downfield[42,43] shift and that the change polymer-like (or helical) aggregate → smaller aggregates occurs with the breakdown of some hydrogen bonds, but also, perhaps, with the formation of other hydrogen bonds among DCA^- anions and water molecules. Thus, the increase in the electron density, if any, is due to the balance between broken and formed hydrogen bonds. It is interesting to note that in the helical model of RbDC the hydroxyl and carboxyl groups are engaged in several hydrogen bonds together with ion–ion and ion–dipole interactions[24] which can influence the chemical shifts, too. Furthermore, the association process alone of the primary micelles to give the larger secondary micelles by means of hydrogen bonds does not modify the packing and the interactions of the NaDC nonpolar faces in the SPC model and hardly explains, therefore, the chemical shifts of the methyl groups and of many other carbon atoms of the steroid skeleton.

Acknowledgment. This work was sponsored in part by the Italian Consiglio Nazionale delle Ricerche-Progetto Finalizzato Chimica Fine e Secondaria.

Registry No. NaDC, 302-95-4; RbDC, 91949-18-7; *p*-xylene, 106-42-3; phenanthrene, 85-01-8; styrene, 100-42-5; 2,3-dimethyl-2-butene, 563-79-1; *trans*-2-butene, 624-64-6.

(42) Kroschwitz, J. I.; Winokur, M.; Reich, H. J.; Roberts, J. D. *J. Am. Chem. Soc.* **1969**, *91*, 5927.
(43) Grover, S. H.; Stothers, J. B. *Can. J. Chem.* **1974**, *52*, 870.
(44) Martin, G. J.; Martin, M. L.; Odiot, S. *Org. Magn. Reson.* **1975**, *7*, 2.